Journal of Colloid and Interface Science 338 (2009) 177–183

Contents lists available at ScienceDirect

Journal of Colloid and Interface Science

www.elsevier.com/locate/jcis

Microstructures and rheological dynamics of viscoelastic solutions in a catanionic surfactant system

Haiqing Yin, Yiyang Lin, Jianbin Huang *

Beijing National Laboratory for Molecular Sciences (BNLMS), State Key Laboratory for Structural Chemistry of Unstable and Stable Species, College of Chemistry and Molecular Engineering, Peking University, Beijing 100871, China

ARTICLE INFO

Article history:
Received 9 March 2009
Accepted 30 May 2009
Available online 6 June 2009

Keywords:
Catanionic surfactant
Viscoelastic solution
Rheology
Wormlike micelles
Dynamic light scattering
Microstructure transition

ABSTRACT

Viscoelastic solutions formed in a catanionic surfactant system of dodecyltriethylammonium bromide (DTEAB)/sodium dodecylsulfate (SDS) at the molar ratio of 27/73 were systematically studied using a combination of rheology and dynamic light scattering (DLS). Wormlike micelles began to form above the total surfactant concentration (C_{total}) of 120 mM by the growth of small cylindrical micelles. Subsequently the system was found to exhibit linear viscoelasticity with characteristic of a Maxwell fluid in the intermediate concentration range of 170–210 mM, which arose from a 3D entangled network of wormlike micelles. At higher surfactant concentrations, a transition from linear micelles to branched structures probably took place. Finally and significantly, the effect of the surfactant headgroup on the rheological property of catanionic surfactant mixtures was discussed.

1. Introduction

Surfactant molecules self-assemble into aggregates in aqueous solutions above the so-called critical micelle concentration (cmc). At low concentrations, the aggregates are generally spherical micelles. In some surfactant systems, long wormlike micelles form at higher concentrations and/or upon addition of salt. For example, hexadecyltrimethylammonium bromide (CTAB) was found to self-assemble into long flexible wormlike micelles by addition of high concentrations of salts or in the presence of hydrophobic counterions [1–3]. The entanglement of these micelles into a transient network can endow viscoelastic properties to the solution, which are analogous to those in flexible polymer solutions. However, unlike chemically-linked polymers, self-assembled wormlike micelles are in equilibrium with their monomers, and can reversibly break and reform under shear. The viscoelasticity of these wormlike micelle networks at low to intermediate frequencies can often be described by a simple Maxwell model [4–7], an interesting rheological behavior which has been actively studied for its great significance from both academic and practical perspectives. The Maxwell response in a surfactant system is considered to be originated from the equilibrium nature of wormlike micelles undergoing dynamic breakage and recombination [3,5].

Aqueous mixtures of anionic and cationic surfactants (referred to as catanionic surfactants) exhibit interesting phase behaviors, which can be controlled by tuning electrostatic interactions between the oppositely charged headgroups. Various microstructures with characteristic geometries ranging from spherical to cylindrical to planar have been extensively studied for this system. Particularly, viscoelastic wormlike micelles formed in catanionic surfactant mixtures are a topic of interest. A series of studies were first performed by Kaler et al. in the mixed system of cetyl trimethylammonium tosylate (CTAT) and sodium dodecylbenzene sulfonate (SDBS) in regard to the formation of wormlike micelle network with increasing SDBS fraction without promotion of salt addition [8] and its microstructural transitions following addition of NaCl and a hydrotropic salt (NaTosylate) [9]. In addition, their group also investigated the synergistic effect on the growth of wormlike micelles in the systems of sodium oleate (NaOA) and trimethylammonium bromide family (C_nTAB) with asymmetric surfactant tail lengths [10]. Alternatively, Hoffmann has observed viscoelastic property in the novel cationic and anionic surfactant system consisting of $C_{14}DMAO/C_6F_{13}CH_2COOH$ and $C_{14}DMAO/CH_3(CH_2)_{11}(CH_2CH_2O)_{2.5}SO_3H$ [11,12]. Nevertheless principles on the formation and transformation of wormlike micelle network in such system are still not fully understood. In this work, we explored viscoelastic solutions formed in a catanionic surfactant system i.e., dodecyltriethylammonium bromide (DTEAB)/sodium dodecylsulfate (SDS) at a fixed molar ratio (27/73). Elongated wormlike micelles were found to be originated from the growth of small cylindrical micelles at lower C_{total} without salt addition. Maxwell fluids were subsequently observed in the intermediate C_{total} range. A systematic study was performed on the physicochemical properties of the Maxwell fluids, including macroscopic and microscopic observations, calculation of characteristic length

* Corresponding author. Fax: +86 10 62751708.
E-mail addresses: jbhuang@pku.edu.cn, JBHuang@chem.pku.edu.cn (J. Huang).

0021-9797/$ - see front matter © 2009 Elsevier Inc. All rights reserved.
doi:10.1016/j.jcis.2009.05.076

scales and free energies as well as temperature effect. In addition, a transformation from linear micelles to branched structures at higher C_{total} was suggested. Finally, the effect of increase in the alkyl chain length of the cationic surfactant headgroup was revealed and possible mechanism was also discussed.

2. Materials and methods

2.1. Materials

Quaternary ammonium bromides were prepared by reaction of 1-bromododecane and the corresponding trialkylamine as described in our previous paper. The abbreviations of the quaternary ammonium bromides are listed as follows: dodecyltriethylammonium bromide (DTEAB), dodecyltripropylammonium bromide (DTPAB) and dodecyltributylammonium bromide (DTBAB). Sodium dodecylsulfate (SDS) was bought from ACROS ORGANICS Co. and used as received. The purity of the surfactant was examined and no surface tension minimum was found in the surface tension curve. The water used was redistilled from potassium permanganate. Sodium bromide was calcined at 500 °C over 6 h before using. The other reagents were products of A.R. Grade.

2.2. Rheological measurements

The rheological properties of samples were measured with a ThermoHaake RS300 rheometer. A cone-plate sensor was used with a diameter of 35 mm and a cone angle of 2°. A sample cover provided with the instrument was used to minimize the change in sample composition by evaporation during the measurement. Frequency sweep measurements were performed in the linear viscoelastic regime determined previously by dynamic strain sweep measurements, in the frequency region from 0.1 to 50 rad s^{-1}. The zero-shear viscosity of the sample was determined from controlled stress measurement by extrapolating the viscosity–shear stress curve to zero shear-rate. All measurements were performed at 25 °C if not specified.

2.3. Dynamic light scattering

DLS measurements were performed on a spectrometer (ALV-5000/E/WIN multiple tau digital correlator) equipped with a Spectra-Physics 2017 200 mW Ar laser (514.5 nm wavelength). The samples were prepared by mixing proper ratios of stock solutions of each surfactant component (pre-filtered through a 0.2 μm syringe filter) and equilibrated at least 48 h before measurements. The measurement was replicated at least three times for each sample, and an average value was calculated. All measurements were performed at 25 °C if not specified.

3. Theoretical considerations

3.1. Maxwell fluids

In the case of a Maxwell fluid, the storage modulus G', the lost modulus G'' and zero viscosity η_0 are given by the following equations:

$$G'(\omega) = \frac{G_0(\omega t_R)^2}{1+(\omega t_R)^2} \tag{1}$$

$$G''(\omega) = \frac{G_0 \omega t_R}{1+(\omega t_R)^2} \tag{2}$$

$$\eta_0 = G_0 t_R \tag{3}$$

where t_R is the relaxation time, ω the frequency and G_0 the plateau modulus. The value of t_R is calculated as the reciprocal of the angular frequency, at which the moduli G' and G'' crossover. G_0 is measured at high frequency where G' reaches a plateau. Also of interest is a linear plot of G'' versus G' which reveals the semicircle characteristic of a Maxwell fluid and known as the "Cole–Cole" plot, which is expressed as

$$G''^2 + \left(G'^2 - \frac{G_0}{2}\right)^2 = \left(\frac{G_0}{2}\right)^2 \tag{4}$$

3.2. Rheology of surfactant wormlike micelles

Cates et al. first theoretically described the rheological behaviors of surfactant wormlike micelles in the semi-dilute regime [5]. In their model, the reversible nature of the micelles allows scission (breaking) and recombination processes to act in addition to micellar reptation. The behavior of the micellar solutions is determined by the ratio of the characteristic breaking time (τ_b) to the characteristic time taken by a micelle of mean contour length L_c to reptate (τ_{rep}). When breaking occurs often over the time-scale of reptation ($\tau_{rep} \gg \tau_b$), the solution behaves as a Maxwell fluid with a single relaxation time (t_R) given by:

$$t_R = (\tau_b \tau_{rep})^{1/2} \tag{5}$$

The rheology of wormlike micelles deviates from Maxwellian behavior at high frequencies, showing an upturn in the viscous modulus G''. These deviations result from a transition in the relaxation mode from reptation at longer time-scales to "breathing" or Rouse modes at short time-scales. G''_{min} is determined as the value of local minimum for G'' at higher frequencies. The ratio G''_{min}/G_0 is another important rheological quantity for wormlike micelles, since it is directly related to the micellar contour length L_c and the scission energy E_{scis} via [6]

$$G''_{min}/G_0 = l_e/L_c \approx \exp(-E_{scis}/2k_BT) \tag{6}$$

Here l_e is the entanglement length, i.e., the average contour length between two entanglement points, which can be determined according to [13]

$$G_0 = k_BT/\xi_M^3 = k_BT/\left(l_e^{9/5} l_p^{6/5}\right) \tag{7}$$

where l_p is the persistence length of the micelles and ξ_M is the network mesh size.

3.3. Dynamic light scattering

In the self-beating mode of dynamic light scattering, the measured time correlation function, $G^{(2)}(\tau,q)$, has the form

$$G^{(2)}(\tau,q) = A(1 + b|g^{(1)}(\tau,q)|^2) \tag{8}$$

where $g^{(1)}(\tau,q)$ is the first-ordered scattered electric field time correlation function; τ, the delay time; A, the experimental baseline; b, a spatial coherence factor which depends on the number of coherence areas generates the signal ($0 < b < 1$); and q, the amplitude of the scattering vector, given by $q = 4\pi n \sin(\theta/2)/\lambda$ with n and θ being the refractive index of the scattering medium and the scattering angle, respectively. The electric field correlation function depends on the Fourier transform of the fluctuating number of the particles or molecules. For a polydisperse system, the field correlation function was analyzed by the constrained regularized CONTIN method [14,15], to yield information on the normalized distribution of the decay constant $G(\Gamma)$ from

$$|g^{(1)}(\tau)| = \int G(\Gamma,q) e^{-\Gamma(q)\tau} d\Gamma \tag{9}$$

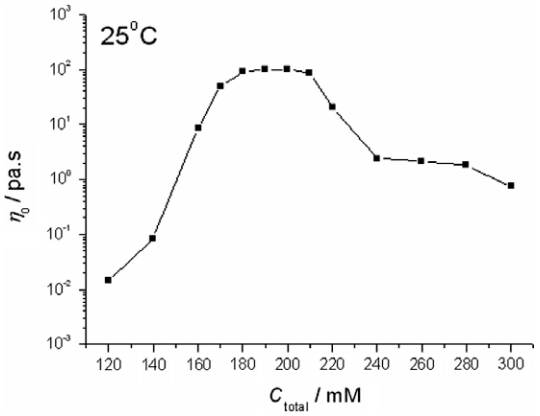

Fig. 1. Variations of zero-shear viscosity (η_0) as a function of total surfactant concentration (C_{total}) for the system of DTEAB/SDS (27/73) at 25 °C.

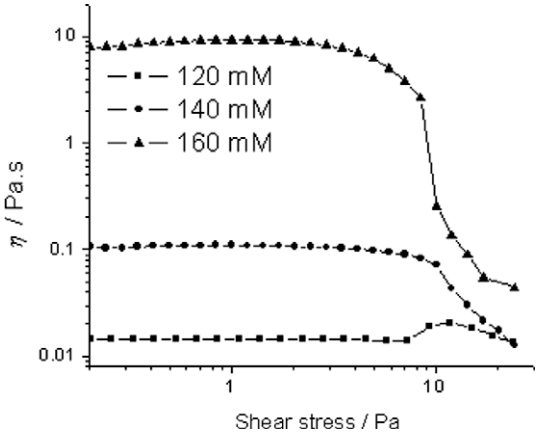

Fig. 2. Variations of apparent viscosity (η) as a function of shear-stress (τ) at C_{total} of 120 mM, 140 mM and 160 mM at 25 °C.

This method is appropriate for the solutions characterized by several relaxations mechanisms. From Eq. (9), the mean relaxation time for each relaxation mode, $\langle\tau_r\rangle$, defined as the area of $|g^{(1)}(\tau,q)|$, is given by

$$\langle\tau_r\rangle = \int G(\Gamma,q)\Gamma d\Gamma \Big/ \int G(\Gamma,q)d\Gamma \tag{10}$$

For a purely diffusive relaxation, $\langle\tau_r\rangle$ is related to the apparent translational diffusion coefficient $D_h = 1/(q^2\tau_r)$. The apparent hydrodynamic radius can then be estimated via the Stokes–Einstein equation

$$R_{h,app} = kT/6\pi\eta D_h \tag{11}$$

where k is the Boltzmann constant and η is the viscosity of water at temperature T.

4. Results and discussion

4.1. Micelle growth with surfactant concentration and formation of viscoelastic solutions

Fig. 1 shows the trend of zero-shear viscosity (η_0) as a function of C_{total} at 25 °C for the mixed system of DTEAB/SDS (molar ratio 27/73). From C_{total} of 120 mM to 160 mM, a dramatic increase in η_0 took place by nearly three orders of magnitude. A plateau in η_0 was then reached from 170 mM to 210 mM and it was followed by a subsequent decrease in η_0 with further increase of C_{total}.

The zero-shear viscosity is relatively low at 120 mM (η_0 = 14.5 mPa s). Variations of apparent viscosity (η) as a function of shear-stress (τ) were measured and plotted in Fig. 2. The system behaved as a Newtonian fluid at lower shear-stresses whereas non-Newtonian behaviors, i.e., shear thickening followed by shear thinning were observed at higher shear-stresses. This phenomenon has been found in many surfactant systems composed of cylindrical micelles [16–18]. As C_{total} increased from 120 to 160 mM, a dramatic increase in η_0 (from 14.5 mPa s to 8.5 Pa s) indicative of micelle growth was observed. Meanwhile the steady rheology for the systems at C_{total} of 140 and 160 mM exhibited different profiles from that at 120 mM (Fig. 2). Following a Newtonian plateau at lower shear-stresses, a shear-thinning behavior took place at higher shear-stresses, which is a characteristic property of wormlike micelles [9].

DLS was employed to track the hydrodynamic properties of the microstructures. Plots of normalized intensity distribution functions of relaxation time $f(\tau)$ at 90° for the samples of 120 mM, 140 mM and 160 mM are shown in Fig. 3a–c, respectively. A single relaxation mode was observed at 120 mM with the apparent hydrodynamic radius ($R_{h,app}$) estimated to be 4.1 nm. Considering the fact spherical micelles formed in the DTEAB/SDS system should have a radius roughly equal to the molecular length of the surfactants (ca. 2 nm), a larger micelle size is therefore consistent with a cylindrical morphology as found from the rheology data. With increase of C_{total}, another mode appeared, which has an equivalent $R_{h,app}$ value of 137 nm and 278 nm for the samples of 140 mM and 160 mM, respectively, which should reflect the formation of elongated wormlike micelles. Thus the DLS data suggest the system underwent a significant growth from small cylindrical micelles into elongated wormlike micelles. It is interesting to note the two populations of micelles coexisted in this case with a relatively large gap in the size distribution.

Fig. 4a shows the results of frequency sweep measurements with change of C_{total}. No apparent viscoelasticity was detected for

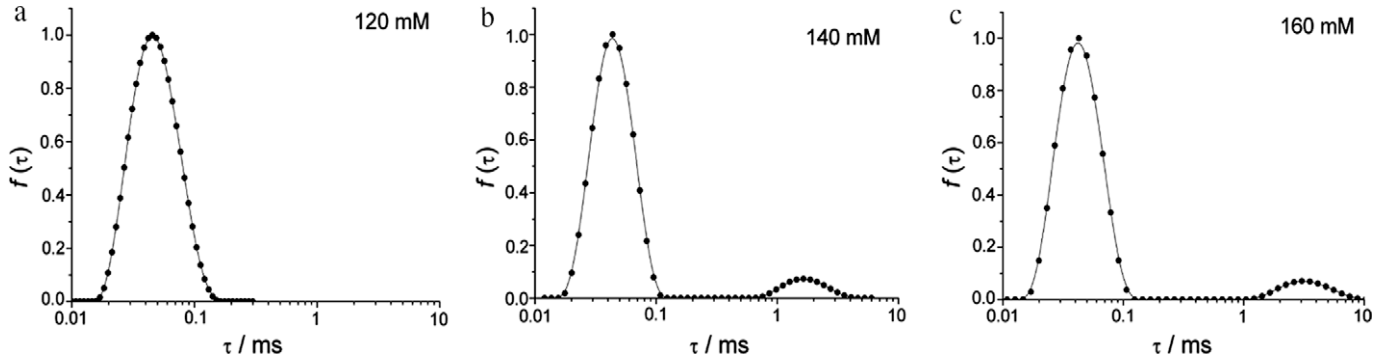

Fig. 3. Plots of normalized intensity distribution functions of relaxation time $f(\tau)$ at 90° for the samples of 120 mM, 140 mM and 160 mM.

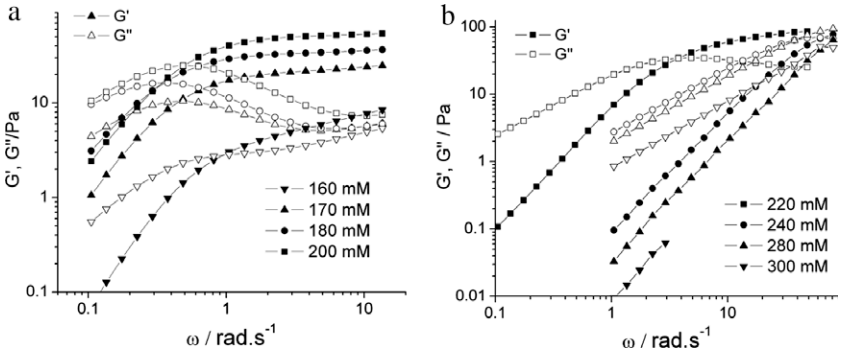

Fig. 4. Dynamic rheological response as a function of C_{total}: 160–200 mM (a) and 220–300 mM (b) for the DTEAB/SDS (27/73) system.

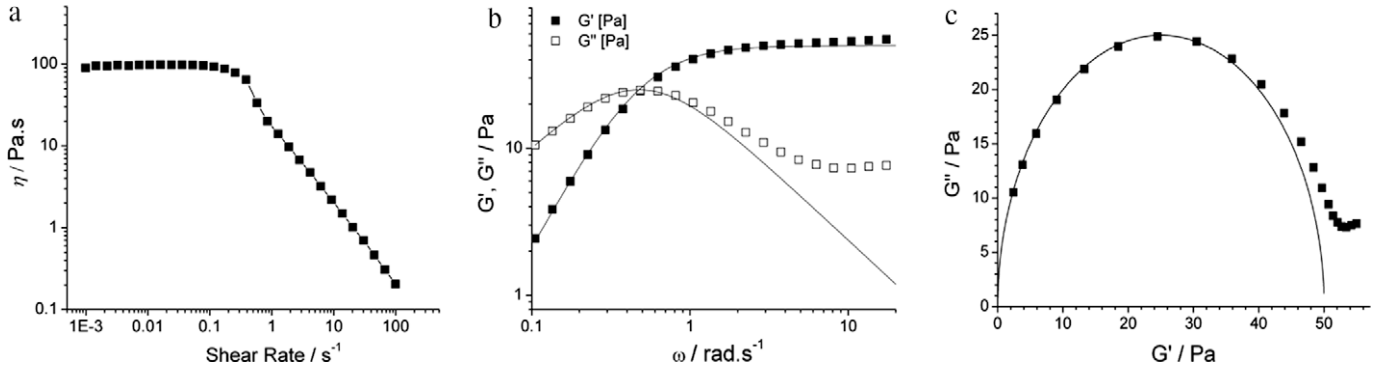

Fig. 5. Rheology of the system DTEAB/SDS (27/73, C_{total} = 200 mM): (a) steady shear rheology (b) dynamic frequency spectrum; (c) Cole–Cole plot (solid lines indicate the best fitting of Maxwell model).

the samples of 120 mM and 140 mM (data were not shown here) whereas the sample of 160 mM started to exhibit viscoelastic response with a spectrum of relaxation times, suggesting the onset of micelle entanglement. Further increase in C_{total} above 170 mM led to a highly viscoelastic fluid with characteristic of Maxwellian behaviors. A systematic study on these solutions was carried out in the following.

4.2. Steady and dynamic rheological properties of Maxwell fluids

Transparent and gel-like solutions were formed in the concentration range of 170–210 mM where η_0 reached a plateau. They can even support its own weight for tens of seconds when standing upside down (Fig. S1). In a typical plot of shear-viscosity vs. shear rate for the system DTEAB/SDS (27/73, C_{total} = 200 mM), two distinct regions were detected (Fig. 5a). At low shear rates, the shear viscosity remained unvaried with the plateau value equal to the zero-shear viscosity η_0 (102 Pa s). As the shear rate increases, a shear thinning behavior can be observed.

A representative plot of frequency sweep measurement, depicting the variations of the storage modulus (G') and loss modulus (G'') with oscillation frequency (ω) is shown in Fig. 5b. The system showed a liquid-like behavior ($G' < G''$) at the low frequency region, but both G' and G'' increased with ω, and solid-like behavior ($G' > G''$) was observed at the high frequency region. This is a typical viscoelastic behavior shown by wormlike micellar solutions. In the low ω region the data points of G' and G'' could be well fitted to the Maxwell equations. Fig. 5c showed the Cole–Cole plot from the data presented in Fig. 5b. A single relaxation time t_R of 2.1 s and a plateau G_0 of 50 Pa thus can be obtained and the value of zero-shear viscosity (102 Pa s) from the product of t_R by G_0 is well consistent with that from the steady rheology measurements. Similar results were also obtained for other viscoelastic samples in the concentration range of 170–210 mM and their rheological parameters (G_0 and t_R) were plotted in Fig. 6. It was found that the maximum of t_R occurred at 180 mM while a progressive increase in G_0 took place until a plateau was reached above 190 mM. It is known that for entangled polymers the plateau modulus G_0 is related to the entanglement density ρ_e by the equation $G_0 = \rho_e k_B T$ [9,19]. Therefore it can be considered the entanglements of wormlike micelles increased with the concentration until 190 mM where ρ_e reached a Maximum, which may suggest another microstructure transition upon further increase of C_{total}.

On the other hand, it should be noted that the experimental points in both Fig. 5b and c deviated the theoretical Maxwell model

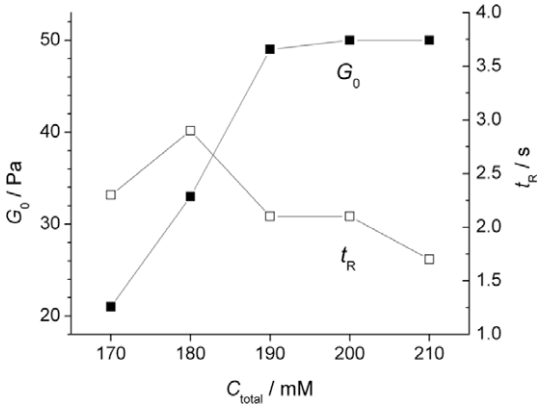

Fig. 6. Variations of G_0 and t_R with change of C_{total} obtained by fitting the Maxwell equations.

at high frequencies, showing an upturn of G''. This phenomenon has been found in many viscoelastic surfactant solutions, which probably resulted from the appearance of Rouse modes or "breathe modes" [8,20–22]. As presented in Eq. (6), the value of G'' at the minimum, i.e., G''_{min} in the frequency sweep measurement provides a relationship between the contour length L_c and entanglement length l_e of the wormlike micelles. l_e then can be calculated via Eq. (7), where the mesh size ξ_M is calculated from G_0. The persistence length l_p in the equation is a intrinsic character of the system and typically a few tens of nanometers for ionic surfactants [23]. Referring to the results in another catanionic surfactant system CTAT/SDBS [9], a value of 20 nm for l_p was assumed to provide a semi-quantitative profile of the DTEAB/SDS system. Thus the mesh size, entanglement length and contour length were estimated to be 43 nm, 72 nm and 450 nm, respectively, showing typical length scales of entangled wormlike micelles.

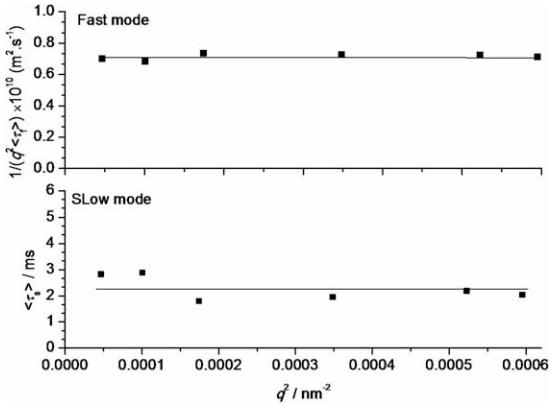

Fig. 8. Dependence of average characteristic time of fast mode and slow mode on the scattering vector q.

4.3. Dynamic light scattering characterizations of Maxwell fluids

DLS experiments were performed on the system of DTEAB/SDS (27/73, C_{total} = 200 mM) at different scattering angles from 30° to 135°. Fig. 7 shows a typical plot of normalized distribution functions of relaxation time $f(\tau)$ at 90°. Several relaxation processes can be clearly observed. The average characteristic time of the fast mode $\langle\tau_f\rangle$ is inversely proportioned to q^2 (Fig. 8), indicating fast mode is a diffusive mode and the apparent diffusion coefficient D_h can be estimated as $1/q^2 \langle \tau_f\rangle$ [24–26]. Using the Stokes–Einstein relationship, a value of 3.5 nm for $R_{h,app}$ was then calculated. Note that the size is quite coincident with that of the small micelles at lower concentrations (120–160 mM), it can be assumed the fast mode probably reflects the diffusive movement of small cylindrical micelles. The domination of the fast mode in the DLS plot indicates that the quantity of these small micelles is still very large in the system.

A distinct slow mode was observed in a longer relaxation timescale (10^3–10^4 ms). Its characteristic time ($\langle\tau_s\rangle$) was found to be independent of the scattering factor q (Fig. 8), which is normally considered to arise from a structural relaxation of a three-dimensional network in the system [27–30]. Interestingly, the $\langle\tau_s\rangle$ value (2.2 s) is well agreed with that of the mechanical relaxation time (t_R = 2.1 s) obtained by the fit of dynamic rheology data to a Maxwell model. We may consider that the slow mode found in DLS should be a global relaxation mode accompanied by the relaxation process of the entangled wormlike micelle network.

In addition to the fast and slow modes, there are several other intermediate modes as shown in Fig. 7. Since these peaks are separated by a factor less than 10, the accuracy of CONTIN fitting method is probably compromised and no simple q dependence is found for these modes (Fig. S2). Actually, these modes are located in a similar time-scale (10^{-1} to 10 ms) as the elongated micelles which were formed above 120 mM. The equivalent $R_{h,app}$ (ca. 100–1000 nm) is also consistent with the typical size of elongated micelles or micelle clusters. Therefore it may be reasonable to assume that the intermediate modes have a diffusive character and are probably related to the diffusive movements of elongated micelles or micelle clusters that are not connected to the network.

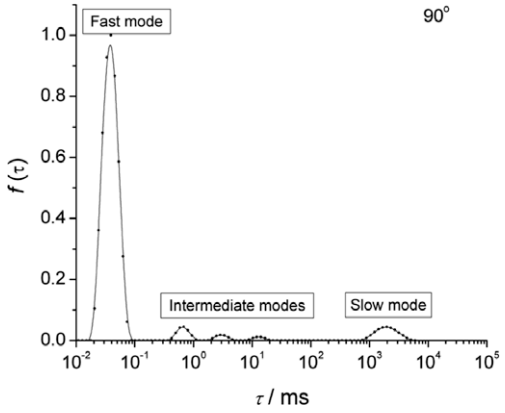

Fig. 7. Plot of normalized distribution functions of relaxation time $f(\tau)$ at 90° for the system DTEAB/SDS (27/73, C_{total} = 200 mM).

Overall the Maxwell fluids are composed of entangled wormlike micelles, separated elongated micelles or micelle clusters, and small cylindrical micelles. It is surprising to note that small micelles with size of several nanometers were found to coexist with much larger entangled wormlike micelle network. Although it is not the first time that multimodal populations of micelles with distinct size difference coexisted in a surfactant system [31–35], such behavior was rarely reported in a viscoelastic solution. The second CMC theory proposed by Israelachvili et al. [36] may give a reasonable explanation to this phenomenon. It is suggested that above the conventional CMC the number of micelles increases with an average constant size as the concentration increases until, above a second critical concentration, refer as the second CMC, the micelles start to increase significantly. The key finding behind this theory is the existence of a energy barrier to overcome for growth of small micelles to occur [37]. Recently Dubin et al. also suggested the coexistence of bimodal micelle species with a relatively large gap in the size distribution is caused by the energetic instability of intermediate structures [32]. On the basis of above experimental and theoretical studies, we assume that there may be a second CMC existing between 120 mM and 140 mM. Above the second CMC, much larger wormlike micelles were formed probably due to the energetically unfavorable formation of intermediate aggregates between the small micelles and wormlike micelles. The small micelles however coexisted with the wormlike micelles as free surfactant molecules coexist with small micelles above the conventional CMC.

4.4. Temperature effect

Temperature effect on the viscoelasticity of the wormlike micelle network was further studied. The variations of rheological parameters for the system DTEAB/SDS (27/73, C_{total} = 200 mM) with temperature change from 15 °C to 30 °C were measured and listed in Table 1. Both the t_R and η_0 were found to drop dramatically with temperature while there is only a little decrease in G_0. Since l_p is almost independent of temperature [38], the same assumed value of l_p was used to calculate corresponding characteristic lengths at

Table 1
Rheological parameters and characteristic length scales for the system DTEAB/SDS (27:73) at different temperatures.

T (°C)	η_0[a] (Pa s)	η_0[b] (Pa s)	G_0 (Pa)	τ_R (s)	G''_{min}/G_0	ξ_M (nm)	l_e[c] (nm)	L_c[c]/ nm
15	1090	1140	57	20	0.050	41	66	1320
20	333	336	56	6.0	0.097	42	69	710
25	102	102	50	2.1	0.16	43	72	450
30	32	28	50	0.56	0.25	44	74	340

[a] η_0 was obtained from the steady rheology results.
[b] $\eta_0 = G_0 t_R$.
[c] Based on the assumed l_p value of 20 nm.

different temperatures which are also listed in Table 1. A remarkable decrease in L_c took place with temperature whereas there was no significant alteration in the mesh size ξ_M and entanglement length l_e. Note that ξ_M and l_e represent characteristic lengths of the entangled micelle network, it can be suggested that the entangled 3D network almost remained integrated within the temperature range studied while a decrease in the contour length of the wormlike micelles should be mainly responsible for the change of rheological response upon temperature increase.

Fig. S3a presents the plot of logt_R versus the reciprocal of the absolute temperature for the system. The plot is linear and demonstrates that the main relaxation time follows an Arrhenius-type behavior of the form

$$t_R = A\exp(E_a/k_BT) \tag{12}$$

where E_a is an activation energy. The activation energy describes the energy that is necessary to move individual micelles in an environment of surrounding micelles [39]. A value of 171 kJ mol^{-1} for E_a obtained from the slope falls into the wide range of E_a values (70-300 kJ/mol) reported for surfactant micellar systems [40–42].

According to Eq. (6), the scission energy E_{scis}, which is required to create two micellar end-caps by breaking a micelle, is related to temperature-dependent variation of G''_{min}/G_0. From the Arrhenius dependence of G''_{min}/G_0 with absolute temperature (Fig. S3b), a value of 165 kJ mol^{-1} for E_{scis} is yielded from the slope. This value is rather high compared to the E_{scis} values reported for conventional ionic surfactants such as CTAB under high ion strength (ca. 40 kJ mol^{-1}) [41,42], indicating formation of elongated micelles is more favored in the catanionic surfactant system probably because of the decreased spontaneous curvature arising from electrostatic interactions between the negatively-charged headgroups. This may generally explain the fact that highly viscoelastic solutions can be formed in a catanionic surfactant system in the absence of salt addition which is usually an essential factor to promote viscoelasticity in an ionic surfactant system.

4.5. Possible microstructure transition at higher surfactant concentrations

As mentioned above, η_0 of the DTEAB/SDS (27/73) system began to decrease after passing a plateau above 210 mM. At the same time, the viscoelasticity of the solution was found to decrease simultaneously with a drop in t_R until the dynamic rheological response almost disappeared above 300 mM (Fig. 4b). Since it was previously revealed the system had a rather high scission energy, branching is expected to occur by the fusion of an end-cap of a micelle with the cylindrical body of another when the scission energy becomes larger than the free energy cost associated with micellar cross-link formation with increase of C_{total}, and it can be energetically favorable because an end-cap disappears [43]. The "cross-links" in the resulting multi-connected micellar network can slide along the micelles and hence serve as stress release points, which accelerate the rate of relaxation process [44]. Such a micellar network will therefore show a reduced viscosity and relaxation time as found in the system. Thus, the drop in η_0 with change of C_{total} probably signifies a shift from linear to branched micelles. As micellar branches increased and dominated the system upon further increase of C_{total}, the viscoelasticity of the solution finally disappeared.

4.6. Effect of alkyl chain of the cationic surfactant headroup

An interesting feature of catanionic surfactant mixtures is their variation and tunability in surfactant headgroup. Herein, rheological properties of different catanionic surfactant systems with varied surfactant headgroup were investigated. Fig. 9 shows variations of η_0 as a function of total surfactant concentration for three catanionic surfactant systems with the same molar ratio (27/73) but increased alkyl chains on the headgroup of the cationic surfactant, i.e., DTEAB/SDS, dodecyltripropylammonium bromide (DTPAB)/SDS and dodecyltributylammonium bromide (DTBAB)/SDS. It is interesting to find that the changes of η_0 with C_{total} for the latter two systems exhibit analogous profiles as that of the DTEAB/SDS system, i.e., firstly a transition from small cylindrical micelles to elongated micelles at lower C_{total}; secondly entangling of wormlike micelles to form a viscoelastic network at intermediate C_{total}; finally a transition from linear micelles to branched structures at higher C_{total}. However, it is noteworthy that the occurrence of viscosity maximum shifted to a lower concentration with increased alkyl chain length from ethyl to butyl. In other words, DTBAB is more efficient in promote micelle elongation than DTEAB and DTPAB. It is believed that formation of wormlike micelles is more favored with increase of alkyl chain length on the surfactant headgroup due to enhanced hydrophobic interactions. Our previous study revealed that vesicle aggregation can be promoted with length increase of the alkyl chains exposed on vesicle surface due to increased inter-vesicular hydrophobic interactions [45]. In this scenario, we consider that the inter-micellar hydrophobic interactions may be strengthened as the alkyl chain length increases from ethyl to butyl so that the free energies required for micelle branching by inter-micellar fusion are also lowered. As a result, micelle entangling and branching occurred at a lower surfactant concentration, respectively, for the system with longer alkyl chain on the cationic surfactant headgroup.

5. Summary

In summary, viscoelastic solutions with characteristic of Maxwell response were formed at semi-dilute concentrations of the DTEAB/SDS mixed system, which arose from the synergistic effect

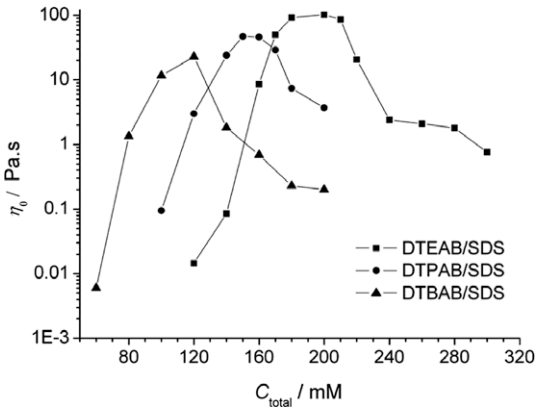

Fig. 9. Variations of η_0 as a function of C_{total} for the systems of DTEAB/SDS, DTPAB/SDS and DTBAB/SDS with the same molar ratio of 27/73 at 25 °C.

of the electrostatic interactions between oppositely charged headgroups. Dynamic light scattering and rheology were shown to be an effective combination to study the process of microstructural evolution in such system. Small cylindrical micelles were found to coexist with the elongated wormlike micelles and even with the subsequently formed micelle network, implying the possible existence of a second CMC. Particularly, the effect of cationic surfactant headgroup on rheological properties was also studied. We hope this work may provide better understanding on viscoelastic solutions in catanionic surfactant systems and promote related practical applications.

Acknowledgments

This work was supported by National Natural Science Foundation of China (20633010, 50521201, 20873001) and National Basic Research Program of China (Grant No. 2007CB936201).

Appendix A. Supplementary material

Macroscopic appearance of the gel-like solution, the intermediate modes of DLS and Arrhenius dependence of characteristic parameter with absolute temperature were presented as Supplementary Materials. Supplementary data associated with this article can be found, in the online version, at doi:10.1016/j.jcis.2009.05.076.

References

[1] S.J. Candau, R. Oda, Colloids Surf. A 183 (2001) 5.
[2] Z. Lin, J.J. Cai, L.E. Scriven, H.T. Davis, J. Phys. Chem. 98 (1994) 5984.
[3] H. Rehage, H. Hoffmann, Mol. Phys. 74 (1991) 933.
[4] M.E. Cates, Macromolecules 20 (1987) 2289.
[5] M.E. Cates, S.J. Candau, J. Phys.: Condens. Matter 2 (1990) 6869.
[6] R. Granek, M.E. Cates, J. Chem. Phys. 96 (1992) 4758.
[7] M.E. Cates, J. Phys.: Condens. Matter 8 (1996) 9167.
[8] R.D. Koehler, S.R. Raghavan, E.W. Kaler, J. Phys. Chem. B 104 (2000) 11035.
[9] B.A. Schubert, E.W. Kaler, N.J. Wagner, Langmuir 19 (2003) 4079.
[10] S.R. Raghavan, G. Fritz, E.W. Kaler, Langmuir 18 (2002) 3797.
[11] J.C. Hao, H. Hoffmann, K. Horbaschek, Langmuir 17 (2001) 4151.
[12] J.C. Hao, H. Hoffmann, K. Horbaschek, J. Phys. Chem. B 104 (2000) 10144.
[13] M. Doi, S.F. Edwards, The Theory of Polymer Dynamics, Clarendon Press, Oxford, 1986.
[14] S.W. Provencher, Biophys. J. 16 (1976) 29.
[15] S.W. Provencher, J. Chem. Phys. 64 (7) (1976) 2772.
[16] S. Hofmann, H. Hoffmann, J. Phys. Chem. B 102 (1998) 5614.
[17] R. Bruinsma, W. Gelbart, A.B. Shaul, J. Chem. Phys. 96 (1992) 7710.
[18] H.Q. Yin, S. Lei, S.B. Zhu, J.B. Huang, J.P. Ye, Chem.–Eur. J. 12 (2006) 2825.
[19] N. Nakajima, J.P. Varkey, Polym. Int. 46 (1998) 298.
[20] D. Varade, K. Ushiyama, L.K. Shrestha, K. Aramaki, J. Colloid Interface Sci. 312 (2007) 489.
[21] P. Fischer, H. Rehage, Langmuir 13 (1997) 7012.
[22] F. Kern, F. Lequeux, R. Zana, S.J. Candau, Langmuir 10 (1994) 1714.
[23] S. May, Y. Bohbot, A.B. Shaul, J. Phys. Chem. B 101 (1997) 8648.
[24] N. Nemoto, M. Kuwahara, M.L. Yao, K. Osaki, Langmuir 11 (1995) 30.
[25] T. Ngai, C. Wu, Y. Chen, Macromolecules 37 (2004) 987.
[26] E. Buhler, C.C. Oelschlaeger, G. Waton, S.J. Candau, J. Phys. Chem. B 108 (2004) 11236.
[27] N. Nemoto, Y. Makita, Y. Tsunashima, M. Kurata, Macromolecules 17 (1985) 2629.
[28] W. Brown, T. Nicolai, S. Hvidt, P. Stepanek, Macromolecules 23 (1990) 357.
[29] M. Adam, M. Delsanti, Macromolecules 18 (1986) 1760.
[30] T. Nicolai, W. Brown, S. Hvidt, K. Heller, Macromolecules 23 (1990) 5088.
[31] V. Weber, T. Narayanan, E. Mendes, F. Schosseler, Langmuir 19 (2003) 992.
[32] P.R. Pinaki, R. Majhi, P.L. Dubin, X.H. Feng, X.H. Guo, F.A.M. Leermakers, C. Tribet, J. Phys. Chem. B 108 (2004) 5980.
[33] M.P. Nieh, S.K. Kumar, R.H. Fernando, R.H. Colby, J. Katsaras, Langmuir 20 (2004) 9061.
[34] A. Bernheim-Grosswasser, R. Zana, Y. Talmon, J. Phys. Chem. B 104 (2000) 4005.
[35] S. May, A. Ben-Shaul, J. Phys. Chem. B 105 (2001) 630.
[36] J.N. Israelachvili, D. Mitchell, B.W. Ninham, J. Chem. Soc., Faraday Trans. 2 (72) (1976) 1525.
[37] G. Porte, Y. Poggi, J. Appel, G. Maret, J. Phys. Chem. 88 (1984) 5713.
[38] N. Willenbacher, C. Oelschlaeger, M. Schopferer, Phys. Rev. Lett. 99 (6) (2007) 068302.
[39] J.D. Ferry, Viscoelastic Properties of Polymers, John Wiley & Sons, New York, 1980.
[40] F. Kern, R. Zana, S.J. Candau, Langmuir 7 (1991) 1344.
[41] F. Kern, F. Lequeux, R. Zana, S.J. Candau, Langmuir 10 (1994) 1714.
[42] J.F.A. Soltero, J.E. Puig, Langmuir 12 (1996) 2654.
[43] T.J. Drye, M.E. Cates, J. Chem. Phys. 96 (1992) 1367.
[44] F. Lequeux, Europhys. Lett. 19 (1992) 675.
[45] H.Q. Yin, Y.Y. Lin, J.B. Huang, J.P. Ye, Langmuir 23 (2007) 4225.